

Enhanced expression of endothelin-1 and endothelin-converting enzyme-1 in acute hypoxic rat aorta

Y. Doi¹, H. Kudo¹, T. Nishino¹, O. Yamamoto², T. Nagata¹, S. Nara¹, M. Morita¹ and S. Fujimoto¹

Departments of ¹Anatomy and ²Dermatology, University of Occupational and Environmental Health, School of Medicine, Kitakyushu, Japan

Summary. Deeply anesthetized male Wistar rats were perfused by Hanks' balanced salt solution bubbled with either 95%air and 5%CO₂ (normoxic group) or 95%N₂ and 5%CO₂ (hypoxic group) from the thoracic aorta for 30 min, and the isolated abdominal aortae from both groups were used for electron microscopy, immunocytochemistry of endothelin (ET)-1 and ET-converting enzyme (ECE)-1, and *in situ* hybridization of preproET-1 mRNA. A remarkable increase in the number of Weibel-Palade (WP) bodies, storage sites of ET-1 and ECE-1, occurred in the hypoxic group when compared to the normoxic group. Immunoreactivities for ET-1 and ECE-1, and signals for preproET-1 mRNA were seen along the endothelia of both groups, but the intensities were significantly elevated in the hypoxic group. The increase in the number of ECE-1 immunoreactive gold particles was noticed especially in WP bodies in the hypoxic group. These findings indicate the enhancement of preproET-1 synthesis in the aortic endothelial cells as well as the acceleration of ET-1 processing in increased WP bodies in such cells in an experimentally hypoxic condition of the rat aortae.

key words: Endothelin-1, Endothelin-converting enzyme-1, Hypoxia, Weibel-Palade body, Rat aorta

Introduction

Since Rubanyi and Vanhoutte (1985) first proposed the involvement of endothelium-derived contracting factors (EDCFs) in vasocontraction of the coronary artery under hypoxic condition, the nature of EDCFs has been much of debate. Yanagisawa et al. (1988) first isolated endothelin (ET)-1 from supernatants of the cultured porcine endothelial cells and suggested that this potent vasocontractive peptide is responsible for mediating hypoxic vasocontraction. Successive

biochemical and pharmacological studies confirmed that hypoxia induces the enhancement of ET-1 release from endothelial cells in vitro (Hieda et al., 1990) and in vivo (Rakugi et al., 1990) in vessels. Subsequently, Kourembanas et al. (1991) described that gene expressions of preproET-1 were elevated in the cultured human umbilical vein endothelial cells under an acute hypoxic condition. Furthermore, Pape et al. (1997) suggested the involvement of this peptide in vasocontraction of the rat aortic rings under acute hypoxia. However, this event has not been confirmed by ultrastructural and immunocytochemical approaches using this vessel in vivo.

Based upon sequence analysis of cDNA for ET-1, Yanagisawa et al. (1988) and Opgenorth et al. (1992) described that the convergence of big ET-1, an intermediate form between preproET-1 and mature ET-1, is performed by ET-converting enzymes (ECEs), which are membrane-bound proteins consisting of ECE-1 and ECE-2. By immunoelectron microscopy using cultured endothelial cells from the human umbilical vein and coronary artery, Russell et al. (1998b) reported that ECE-1 is localized in Weibel-Palade (WP) bodies. Furthermore, these inclusions are a storage site of ET-1 in endothelial cells of a variety of vessels (Sakamoto et al., 1993; Doi et al., 1996; Russell et al., 1998a; Kayashima et al., 1999; Kiyonaga et al., 2001). On this basis, it is reasonable to assume that WP bodies are sites for ET-1 processing and ET-1 release in a manner of regulated pathway.

WP bodies are segregated from the trans-Golgi network and include variety of vasoactive substances such as histamine (Kagawa and Fujimoto, 1987; Ueda et al., 1992; Doi et al., 1995), and calcitonin gene-related peptide (CGRP) (Ozaka et al., 1997; Doi et al., 2001) in addition to ET-1. Dynamic changes in frequency of WP bodies under a variety of physiological and pathological vascular conditions were already observed. Meyrick and Reid (1978) and Sakamoto et al. (1993) demonstrated that chronic hypoxia induces an increase in the number of WP bodies in the rat pulmonary artery and in the rabbit umbilical vein, respectively. However, these events have not been confirmed in acute hypoxic

Offprint requests to: Yoshiaki Doi, Department of Anatomy, University of Occupational and Environmental Health, School of Medicine, 1-1 Iseigaoka, Yahatanishi-ku, Kitakyushu 807-8555, Japan. Fax: +81 (93) 692-0121. e-mail: y-doi@med.uoeh-u.ac.jp

conditions.

On these grounds, the present experiments were focused on numerical changes of WP bodies, on expressions of preproET-1 mRNA, and on immunoreactivities for ET-1 and ECE-1 in acute hypoxic rat aortae. The purpose of this study is to throw lights on the roles of WP bodies as storage and processing sites of ET-1 in the aortic vasoconstriction under an experimentally-induced acute hypoxic condition.

Materials and Methods

Animals

Male adult Wistar rats weighing 280 ± 20 g were used for the present study. As for the care and use of the animals utilized for this study, the authors followed the Guiding Principles for the Care and Use of Animals approved by the University of Occupational and Environmental Health in accordance with the principles of the declaration of Helsinki (1983). Animals were deeply anesthetized with an intraperitoneal injection of 5 mg pentobarbital per 100 g body weight and perfused from the left ventricle with heparinized Hanks' balanced salt solution (HBSS) for 5 min at 37°C . A Teflon catheter (QUIK-CATH 18G; Travenol, Deerfield, IL, USA) was then inserted into the thoracic aorta and ligated into place. Animals were perfused with normoxic (95% air, 5% CO_2) or hypoxic (95% N_2 , 5% CO_2) HBSS from the catheter for 30 min at a constant flow rate of 4.0 ml/min using a peristaltic pump (Masterflex; Cole-Parmer, Chicago, IL, USA), and provided for the following experiments.

Tissue preparation for electron microscopy

For conventional transmission electron microscopy, both normoxic perfused rats (normoxic group: 10 rats) and hypoxic perfused ones (hypoxic group: 10 rats) were successively perfused from the catheter with a mixture of 2.0% paraformaldehyde (PFA) and 2.5% glutaraldehyde (GA) in 0.1M phosphate buffer for 5 min at 4°C . The abdominal aortae above the left renal artery branch were isolated from both groups and then immersed in the same fixative for 2 h at 4°C , postfixed in 1% osmium tetroxide in the same buffer for 2 h at 4°C , dehydrated in a graded concentration of acetone series, and embedded in epoxy resin. Ultrathin sections were made on an MT-X ultramicrotome (Ventana Medical Systems, Tucson, AZ, USA), stained with 5% uranyl acetate and lead citrate, and examined in a JEM 1210 transmission electron microscope.

Tissue preparation for light microscopy

For detection of immunoreactivities for ET-1 and ECE-1 and signals for preproET-1 mRNA, animals of both groups (10 rats each) were perfused from the catheter with 4.0% PFA in 0.1M phosphate buffer for 5

min at 4°C . The abdominal aortae were isolated from both groups and then immersed in the same fixative for 72 h at 4°C , dehydrated in a graded concentration of ethanol series, and embedded in paraffin (Merck, Darmstadt, Germany).

Polyclonal antiserum against rat ECE-1

Rat ECE-1 antiserum was raised in rabbits against a synthetic peptide corresponding to amino acid sequence 461-474 (Shimada et al., 1994) of rat ECE-1 coupled to keyhole limpet hemocyanin (Sigma, St. Louis, MO). The antiserum was screened by ELISA and purified using an affinity column. To determine specificity of the antiserum, Western blotting was performed using the rat lung membrane fractions.

Light microscopic immunocytochemistry

Paraffin-embedded sections of approximately 5 μm thickness were deparaffinized, rinsed briefly in 0.1M phosphate-buffered saline (PBS), digested with 0.4% pepsin in distilled water containing 0.01N HCL for 40 min, treated with 0.3% H_2O_2 in absolute methanol to block the endogenous peroxidase activity, and thoroughly washed in 0.1M PBS. Sections were incubated with normal goat serum for 15 min followed by incubation in a humid chamber with the mouse anti-ET-1 monoclonal antibody against the c-terminal of ET-1 (clone number, 8H10; Yamasa, Chiba, Japan), which is detectable for ET-1 only, at a concentration of 10 $\mu\text{g}/\text{ml}$ in PBS, or the rabbit anti-rat ECE-1 antiserum at a concentration of 2 $\mu\text{g}/\text{ml}$ in PBS for 16 h at 4°C , respectively. Specificity of the anti-ECE-1 antiserum was confirmed by the preabsorption test with the synthetic peptide corresponding to amino acid sequence 461-474 of rat ECE-1. After rinsing in 0.1M PBS, sections were immunostained using the indirect immunoperoxidase method (Histfine Simple Stain PO Kit, Nichirei, Tokyo, Japan), and the peroxidase complex was visualized by treatment with a freshly prepared tetrahydrochloride diaminobenzidine (DAB; 0.1 mg/ml) solution with 0.01% H_2O_2 for 5 min.

Immunoelectron microscopy

For immunoelectron microscopy, animals were perfused from the catheter with periodate-lysine-PFA (PLP; Mclean and Nakane, 1974) for 5 min at 4°C . The aortae were isolated from both groups (5 rats each) and then immersed in the same fixative for 6 h at 4°C , dehydrated in a graded concentration of ethanol series, and embedded in epoxy resin. After non-specific bindings were blocked with 1% bovine serum albumin (BSA) in 0.1M PBS, ultrathin sections of gold interference colors made on the ultramicrotome were immunolabeled with the anti-rat ECE-1 antiserum at a concentration of 1 $\mu\text{g}/\text{ml}$ in PBS for 4 h at room temperature. Sections were washed in 0.1M PBS,

blocked in 1% BSA in 0.1M PBS for 20 min, incubated with the goat anti-rabbit IgG-coated 15 nm colloidal gold (Ultra Biosols, Liverpool, UK) with a dilution of 1:100 in 0.1% BSA in 0.1M PBS for 1 h at room temperature, and rinsed in 0.1M PBS. Specificity of the above immunostainings was confirmed by substituting the primary antibodies for the normal rabbit sera or PBS.

In situ hybridization for preproET-1 mRNA

The template cDNA for PCR was synthesized from poly (A)⁺ RNA of normal rat liver according to the procedure described by Kudo et al. (1999). Oligonucleotides for rat preproET-1 cDNA synthesis and PCR amplification were performed according to the method described by Fukushima et al. (2000). Digoxigenin (DIG)-labeled antisense and sense RNA probes were prepared with SP6 RNA polymerase using a DIG RNA labeling kit (Boehringer Mannheim, Mannheim, Germany) according to instructions provided by the manufacturer.

To detect preproET-1 mRNA, tissue sections adjacent to those used for the above immunocytochemical stainings for both ET-1 and ECE-1 were stained with DIG-labeled cRNA probe *in situ* hybridization technique as described by Kudo et al. (1999). To visualize the signals for preproET-1 mRNA, sections were immunoreacted with the peroxidase-conjugated sheep IgG-F(ab')₂ fragment to DIG (Boehringer Mannheim, Mannheim, Germany). After rinsed with TNT buffer containing 0.1M Tris-HCl (pH7.5), 0.15M NaCl, and 0.05% Tween 20, the peroxidase immunoreactivities were amplified with a TSA-Indirect ISH kit (New England Nuclear, Boston, MA, USA). Sections were followed by treatment with freshly prepared DAB (0.5 mg/ml) solution with 0.01% H₂O₂ for 10 min.

To assess specificity of *in situ* hybridization signals, two negative control procedures were performed. First, RNA was digested in randomly selected sections by preincubation with the above RNase A buffer. Second, the digoxigenin-labeled sense RNA probes were hybridized in parallel to the antisense RNA probes in all cases.

Semiquantification of ET-1 and ECE-1 immunoreactivity and preproET-1 signal

To quantify immunoreactivities for ET-1 and ECE-1 and signals of preproET-1 mRNA along the abdominal aortic endothelia, the following procedures were carried out using four randomly-chosen rats from the normoxic and the hypoxic groups: The total length of each endothelium was divided into several areas of the same extension, and the immunoreactive intensities and signals obtained from five randomly-chosen areas were measured using a microscope (BX50, Olympus, Tokyo, Japan) equipped with a Polaroid Digital camera (Nippon Polaroid, Tokyo, Japan) and NIH image analysis

software (version 1.61).

Quantitative evaluation of Weibel-Palade body

Quantitative analyses on the number and total area of WP bodies per 100 μm^2 endothelial cells area were carried out with an image-analysing device (Nikon Cosmosone 1S, Tokyo, Japan), using twenty electron micrographs of the abdominal aortae from normoxic and hypoxic groups at a final magnification of x40,000 each. The number of WP bodies per each endothelial cell was counted directly in the electron micrographs, and the areas of each endothelial cell and the total areas occupied by WP bodies per each endothelial cell were measured. For statistical comparisons between data from the normoxic and hypoxic groups, Student's *t*-test for unpaired comparisons were used.

Quantitative analysis of immunoreactive gold particles for ECE-1

Quantitative analyses on the number of ECE-1 immunoreactive gold particles on WP bodies as well as on cytosol near the endothelial cell membrane per 1.0 μm^2 endothelial area were carried out with the image-analysing device using randomly selected immunoelectron micrographs from the normoxic and hypoxic groups (6 micrographs each).

Results

Electron microscopy

Endothelial cells of the abdominal aortae in the normoxic group contained a considerable number of WP bodies, and the perfusion with normoxic HBSS from the catheter did not result in any significant ultrastructural changes, such as swelling and degranulation of these inclusions (Fig. 1).

On the other hands, the remarkable increase in the number of WP bodies occurred in endothelial cells of the hypoxic group (Fig. 2). Immature forms of WP bodies often existed near the Golgi apparatus (Fig. 3). A considerable number of WP bodies undergoing degranulation (Fig. 4A) or aggregating near the apical endothelial cell membrane (Fig. 4B) were seen in the endothelial cells of the hypoxic group.

Concentration of WP bodies

The quantitative data are shown in Figure 5: The number (Fig. 5A) and the total area (Fig. 5B) of WP bodies per 100 μm^2 endothelial cell area significantly increased in the hypoxic group when compared to those in the normoxic group.

Light microscopic immunocytochemistry

Immunoreactivities for ET-1 in the normoxic (Fig.

6A) and the hypoxic (Fig. 6B) groups were localized along the endothelia, but the staining intensity appeared to be more pronounced in the hypoxic group. Immunoreactivities for ECE-1 in both groups were also localized along the endothelia showing the enhanced intensities in the hypoxic group (Figs. 7A,B).

Immunoelectron microscopy

By immunoelectron microscopy using the post-embedding method, ECE-1 immunoreactive gold particles in the normoxic group were preferentially localized in WP bodies and along the endothelial cell membrane (Fig. 8A). The gold particles in WP bodies much increased in the number in the hypoxic group when compared to those in the normoxic group (Fig. 8B).

Few or no immunoreactivities were seen in the endothelial cells when the primary antibody was replaced for PBS (Fig. 8C).

Quantitative analysis of immunoreactive gold particles

The number of ECE-1 immunoreactive gold particles on WP bodies per $1.0 \mu\text{m}^2$ endothelial area significantly increased in the hypoxic group when compared to that in the normoxic group (Fig. 9A), while

there existed no significant differences between both groups in number of the gold particles on the cytosol near the endothelial cell membrane (Fig. 9B).

In situ hybridization

PreproET-1 mRNA signals were detectable from the endothelium of both normoxic and hypoxic groups (Figs. 10A,C). However, the signal intensities appeared to be more pronounced in the hypoxic group (Fig. 10C). Hybridization using sense probe in adjacent sections showed no detectable signals from the aortae of both groups (Fig. 10B,D).

Figure 11 demonstrates semiquantitative data of immunoreactivities for ET-1 and ECE-1 and signals for preproET-1 mRNA in five randomly selected areas of each endothelium from both the normoxic and hypoxic groups (4 rats each). As shown in this figure, immunoreactivities for ET-1 (Fig. 11A) and ECE-1 (Fig. 11B), and signals for preproET-1 mRNA (Fig. 11C) were significantly elevated in the hypoxic group when compared to those in the control group, respectively.

Discussion

In the short-term hypoxic rat aorta, the remarkable increase in the number of WP bodies occurred in

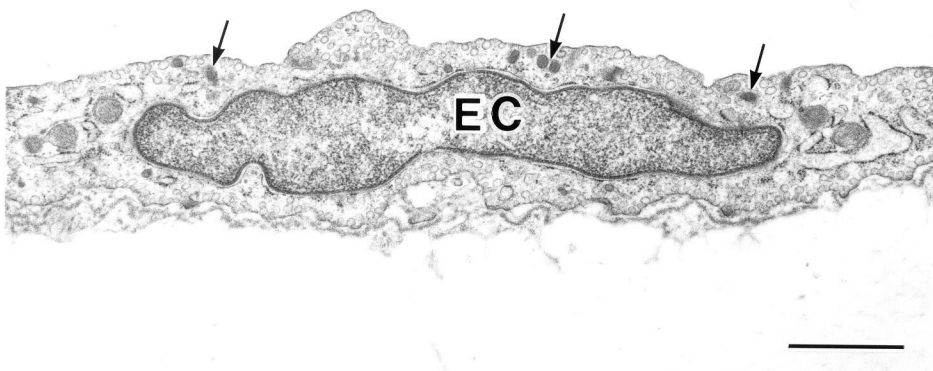


Fig. 1. An endothelial cell (EC) of abdominal aorta in the normoxic group contains a considerable number of WP bodies (arrows). Bar: 1 μm .

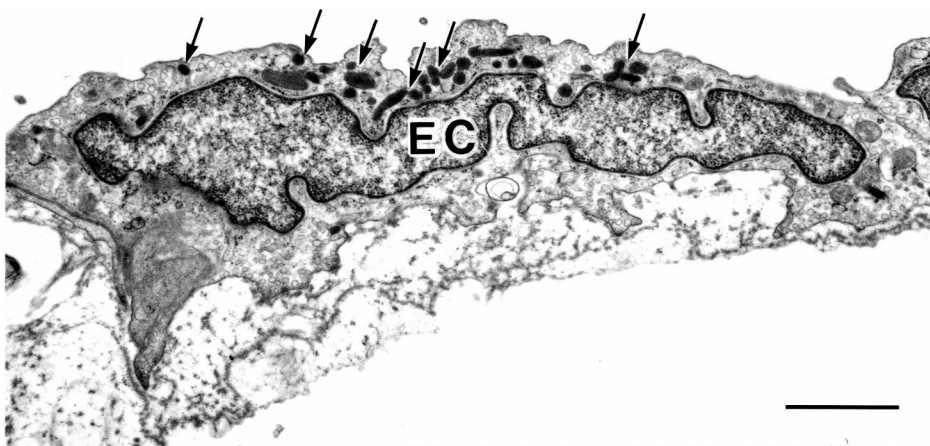


Fig. 2. A remarkable increase in the number of WP bodies (arrows) occurs in an endothelial cell (EC) of the hypoxic group. Bar: 1 μm .

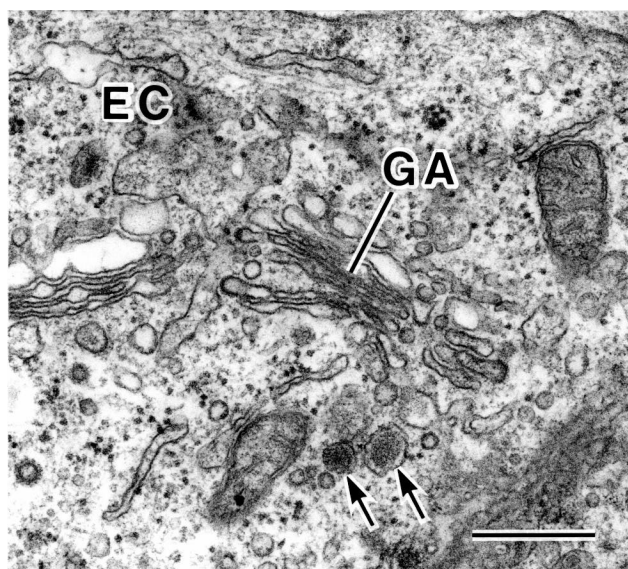


Fig. 3 Segregation of immature forms of WP bodies (arrows) is seen in proximity of the Golgi apparatus (GA) in an endothelial cell (EC) of the hypoxic group. Bar: 500 nm.

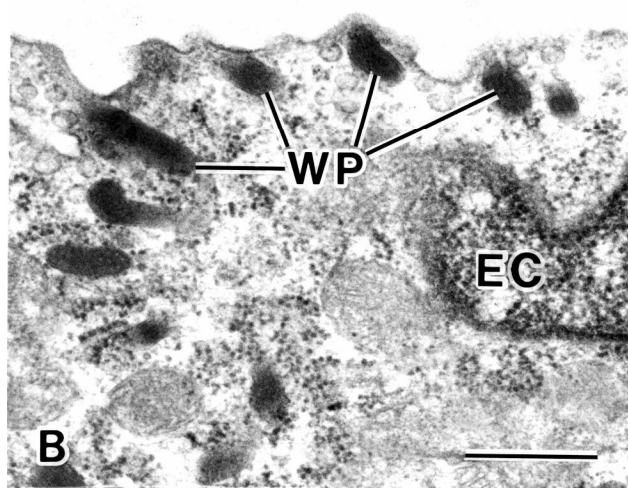
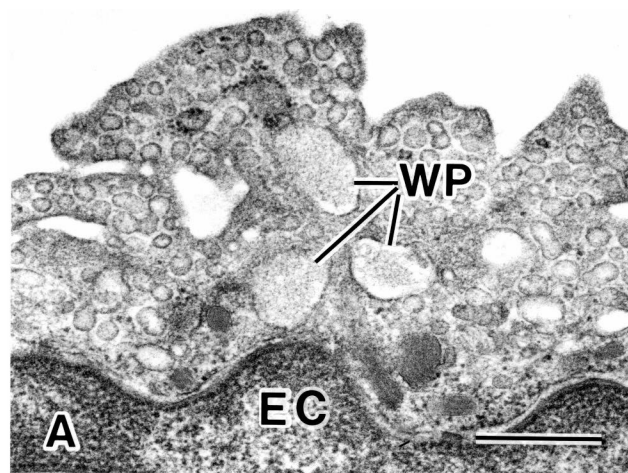


Fig. 4 Some WP bodies undergo degranulation (WP in **A**) and aggregate near the apical cell membrane (WP in **B**) in endothelial cells (ECs) of the hypoxic group. Bars: 500 nm.

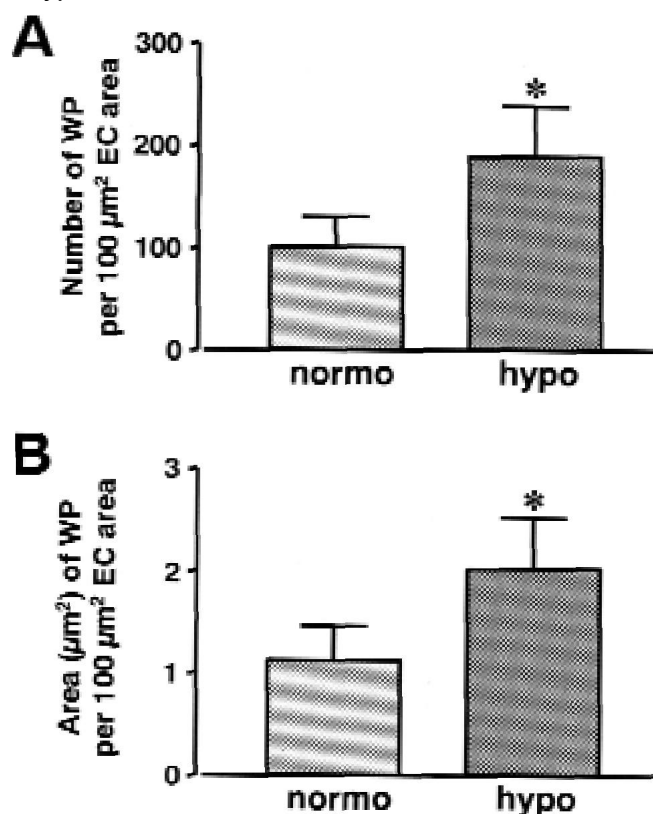


Fig. 5 Quantification of concentrations of WP bodies in endothelial cells. Number (**A**) and total area (**B**) of WP bodies (WP) per 100 μm^2 endothelial cell (EC) area significantly increase in the hypoxic group (hypo) when compared to those in the normoxic group (normo). Bars: mean \pm SD. *: $p < 0.01$.

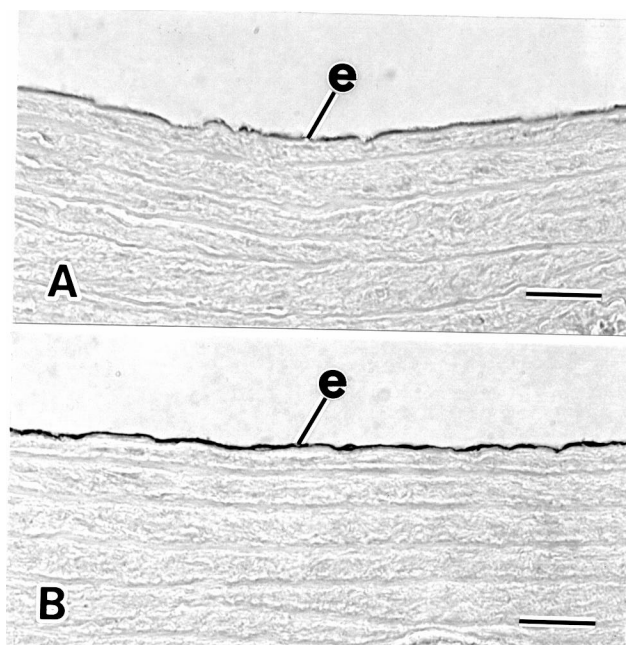


Fig. 6 Immunoreactivity for ET-1 in abdominal aorta of the normoxic (**A**) and hypoxic (**B**) groups. The immunoreactivity is preferentially localized along the endothelia (e) in both groups, but immunoreactive intensity is much elevated in the hypoxic group (**B**) when compared to that of the normoxic group (**A**). Bars: 10 μm .

endothelial cells by active segregation in the Golgi apparatus. In addition, the degranulation and aggregation of these inclusions to the endothelial cell membrane was frequently encountered. It has been already reported that certain physiological conditions such as chronic hypoxia (Meyrick and Reid, 1978; Kagawa and Fujimoto, 1987), heavy metal intoxication (Yoshizuka et al., 1990; Doi et al., 1996) and administration of LH-RH agonist (Hamasaki et al., 1995) induce a transient increase in the number of WP bodies. Since the first description of WP bodies (Weibel and Palade, 1964), successive studies revealed that WP bodies are a storage site for a variety of bioactive substances such as von Willebrand factor (Ewenstein et al., 1987; Kagawa and Fujimoto, 1987), p-selectin (McEver et al., 1987; Bonfanti et al., 1989), ET-1 (Sakamoto et al., 1993; Doi et al., 1996; Kayashima et al., 1999), nitric oxide synthase (Fukuda et al., 1995), and CGRP (Ozaka et al., 1997; Doi et al., 2001). According to Sakamoto et al. (1993), Doi et al. (1996) and Kayashima et al. (1999), WP bodies are involved in the extracellular release of ET-1 from endothelial cells in a manner of regulated pathway. Recently, Russell et al. (1998b) revealed the localization of ECE-1, which converts big ET-1 to ET-1, in WP bodies of the cultured human umbilical vein by immunoelectron microscopy, implying that WP bodies are a processing site of ET-1 in endothelial cells.

In the present immunocytochemistry, it was revealed that acute hypoxia induces enhanced immunoreactivities for ET-1 and ECE-1 in the abdominal aortic endothelium. Our immunoelectron micrographs indicated that the localization of ECE-1 immunoreactive

gold particles in WP bodies much more increased in the number in the hypoxic group when compared to the normoxic group. Since the ET-1 antibody used in the present immunocytochemistry does not detect big ET-1, it is apparent that enhanced immunoreactivity for ET-1 does not reflect that for big ET-1. Taking the above into consideration, it is reasonable to assume that ET-1 processing and release are enhanced in WP bodies, which increased in the number in an acute hypoxic condition.

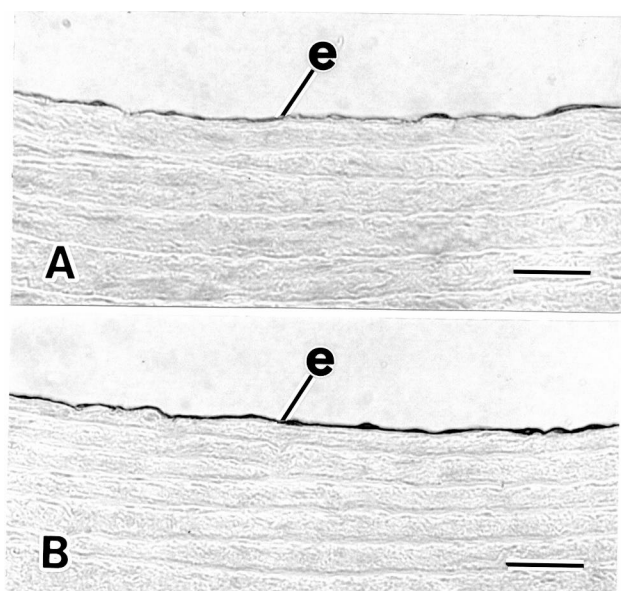


Fig. 7. Immunoreactivity for ECE-1 in abdominal aorta of the normoxic (A) and hypoxic (B) groups. The immunoreactivity is preferentially localized along the endothelia (e) in both groups, but immunoreactive intensity is much elevated in the hypoxic group (B) when compared to that of the normoxic group (A). Bars: 10 µm.

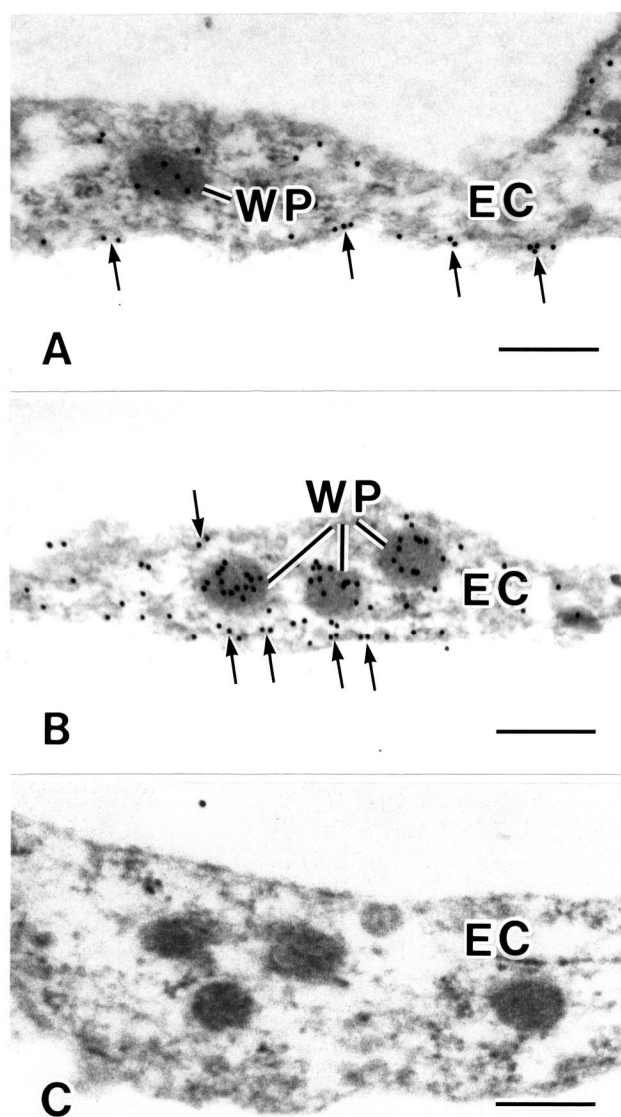


Fig. 8. Immunoreactive gold particles for ECE-1 localize in WP bodies as well as in cytosol near the cell membrane (arrows) of an endothelial cell (EC) in the normoxic group (A). Increase in the number of the immunoreactive gold particles is noticed in WP bodies but is not in cytosol near the cell membrane (arrows) of an endothelial cell (EC) in the hypoxic group (B). Few or no immunoreactive gold particles are seen when the primary antibody is replaced by PBS in an endothelial cell (EC) of the hypoxic group (C). Bars: 200 nm.

We also demonstrated that immunoreactivities for ET-1 and signals for preproET-1 mRNA were enhanced in the acute hypoxic endothelium. This may imply the

enhancement of ET-1 synthesis as well as processing of this peptide in WP bodies. This assumption argues for the previous biochemical data indicating the elevation of ET-1 concentrations in the perfusate obtained from the hypoxic rat mesenteric arteries (Rakugi et al., 1990), as well as in the medium obtained from cultured human umbilical vein endothelial cells (HUVEC) exposed to hypoxia (Hieda et al., 1990). Furthermore, elevated expressions of preproET-1 mRNA from the cultured HUVEC exposed to hypoxia were assayed using Northern Blotting (Kourembanas et al., 1991). Our immunocytochemistry and *in situ* hybridization also argue for the above data. Since a recent paper suggested that gene expressions of preproET-1 and ECE-1 are independently regulated (Corder and Barker, 1999), further studies are necessary to elucidate whether expressions of ECE-1 mRNA are elevated in a hypoxic condition.

In conclusion, WP bodies, which increased in the number in endothelial cells of the acute hypoxic aorta, are involved in the enhancement of ET-1 processing and release, and this phenomenon leads to the ET-1-mediated vasocontraction.

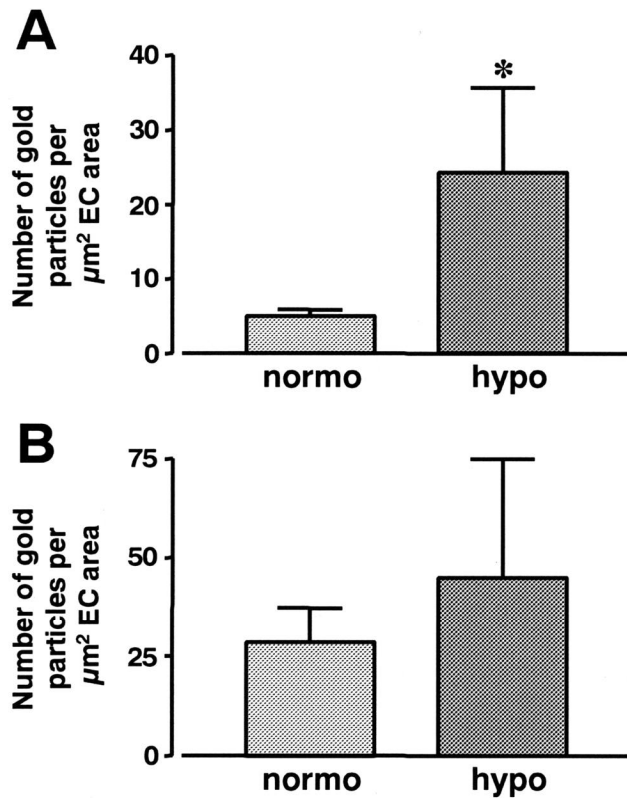


Fig. 9. Quantification of number of immunoreactive gold particles for ECE-1. Number of the gold particles on WP bodies per $1.0 \mu\text{m}^2$ endothelial area (**A**) significantly increase in the hypoxic (hypo) group when compared to that in the normoxic (normo) group (**A**). On the other hands, number of the gold particles on the cytosol near the endothelial cell membrane (**B**) shows no significant differences between the normoxic (normo) and the hypoxic (hypo) groups (**B**). Bars: mean \pm SD. *: $p < 0.01$.

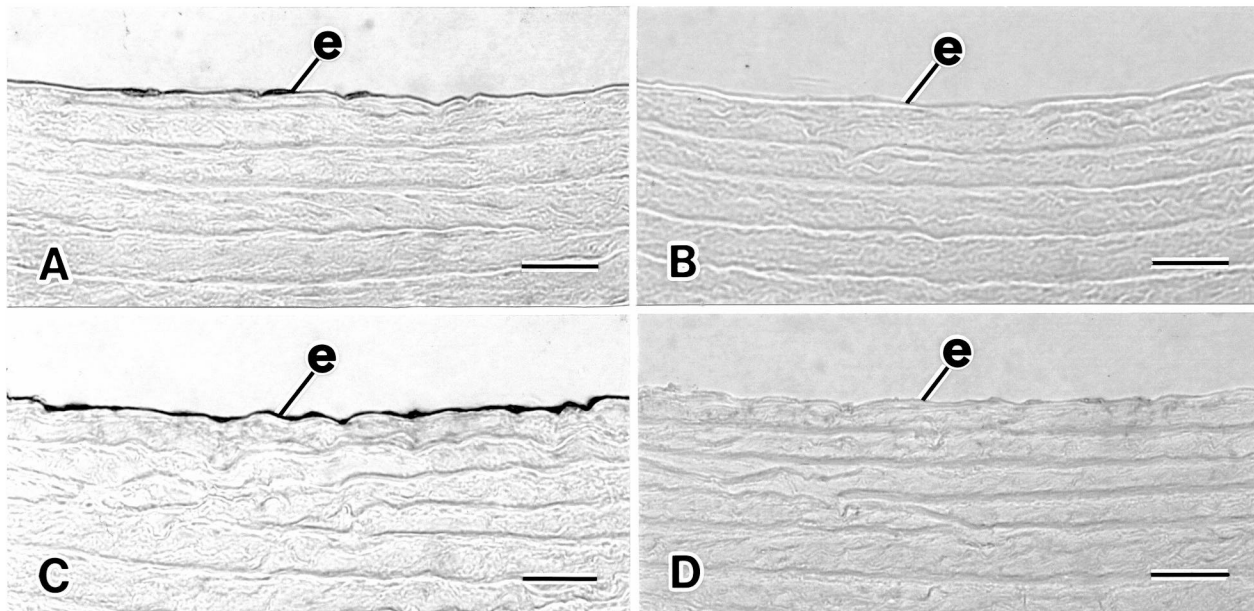


Fig. 10. PreproET-1 mRNA signals are detectable from the endothelia (e) of normoxic (**A**) and hypoxic (**C**) groups, respectively. However, the signal intensity much increases in the hypoxic group (**C**). Hybridization using sense probes in adjacent sections shows no detectable signals from the normoxic (**B**) and the hypoxic (**D**) groups. Bars: $10 \mu\text{m}$.

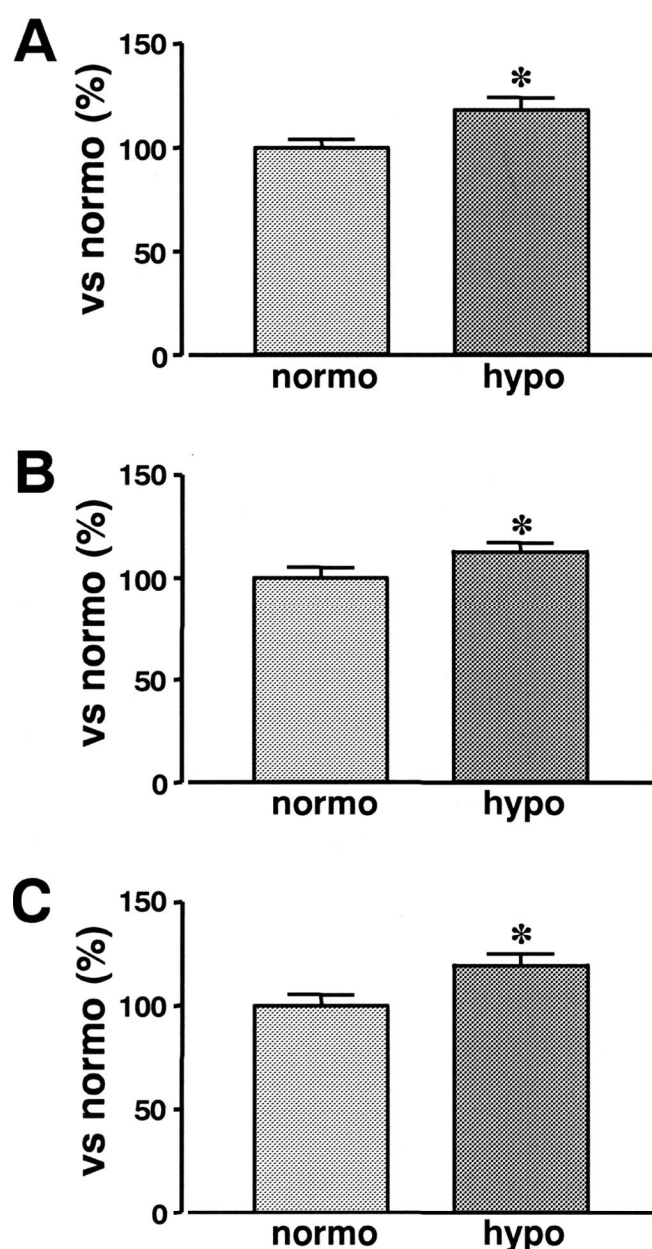


Fig. 11. Semi-quantification of immunoreactive intensity for ET-1 (A) and ECE-1 (B), and signal intensity for preproET-1 mRNA (C). Both immunoreactive and signal intensities are significantly elevated in the hypoxic (hypo) group when compared to those in the normoxic (normo) group. Bars: mean \pm SD. *: $p < 0.01$.

Acknowledgements. We thank Dr. Takatoshi Ozaka for his participation in earlier phases of this project, Mr. Mitsuru Yokoyama for his photographic work, and Ms. Toyono Nobukuni for typing the manuscript.

References

Bonfanti R., Furie B.C., Furie B. and Wagner D.D. (1989). PADGEM (GMP140) is a component of Weibel-Palade bodies of human

- endothelial cells. *Blood* 73, 1109-1112.
- Corder R. and Barker S. (1999). The expression of endothelin-1 and endothelin-converting enzyme-1 (ECE-1) are independently regulated in bovine aortic endothelial cells. *J. Cardiovasc. Pharmacol.* 33, 671-677.
- Doi Y., Ozaka T., Katsuki M., Fukushige H., Toyama E., Kanazawa Y., Arashidani K. and Fujimoto S. (1995). Histamine release from Weibel-Palade bodies of toad aortas induced by endothelin-1 and sarafotoxin-S6b. *Anat. Rec.* 242, 374-382.
- Doi Y., Ozaka T., Fukushige H., Furukawa H., Yoshizuka M. and Fujimoto S. (1996). Increase in number of Weibel-Palade bodies and endothelin-1 release from endothelial cells in the cadmium-treated rat thoracic aorta. *Virchows Arch.* 428, 367-373.
- Doi Y., Kudo H., Nishino T., Kayashima K., Kiyonaga H., Nagata T., Nara S., Morita M. and Fujimoto S. (2001). Synthesis of calcitonin gene-related peptide (CGRP) by rat arterial endothelial cells. *Histol. Histopathol.* 16, 1073-1079.
- Ewenstein B.M., Warhol M.J., Handin R.I. and Pober J.S. (1987). Composition of the von Willebrand factor storage organelle (Weibel-Palade body) isolated from cultured human umbilical vein endothelial cells. *J. Cell Biol.* 104, 1423-1433.
- Fukuda S., Takaichi S., Naritomi H., Hashimoto N., Nagata I., Nozaki K. and Kikuchi H. (1995). Ultrastructural localization and translocation of nitric oxide synthase in the endothelium of the human cerebral artery. *Brain Res.* 696, 30-36.
- Fukushige H., Doi Y., Kudo H., Kayashima K., Kiyonaga H., Nagata T., Itoh H. and Fujimoto S. (2000). Synthesis and receptor sites of endothelin-1 in the rat liver vasculature. *Anat. Rec.* 259, 437-445.
- Hamasaki K., Doi Y., Sakamoto Y., Kashimura M. and Fujimoto S. (1995). The contraction of small arteries in the perimetrium by presurgical medication with the luteinizing hormone-releasing hormone agonist to patients with leiomyomas: an electron and immunoelectron microscopy. *Fukuoka Acta Med.* 86, 389-397.
- Hieda H.S. and Gomez-Sanchez C.E. (1990). Hypoxia increases endothelin release in bovine endothelial cells in culture, but epinephrine, norepinephrine, serotonin, histamine and angiotensin II do not. *Life Sci.* 47, 247-251.
- Kagawa H. and Fujimoto S. (1987). Electron-microscopic and immunocytochemical analyses of Weibel-Palade bodies in the human umbilical vein during pregnancy. *Cell Tissue Res.* 249, 557-563.
- Kayashima K., Doi Y., Kudo H., Kiyonaga H. and Fujimoto S. (1999). Effects of endothelin-1 on vasoactivity and its synthesis, storage, and acting sites in the rat superior mesenteric vasculature: an ultrastructural and immunocytochemical study. *Med. Electron Microsc.* 32, 36-42.
- Kiyonaga H., Doi Y., Karasaki Y., Arashidani K., Itoh H. and Fujimoto S. (2001). Expressions of endothelin-1, fibronectin and interleukin-1 of human umbilical vein endothelial cells under prolonged culture. *Med. Electron Microsc.* 34, 41-53.
- Kourembanas S., Marsden P.A., McQuillan L.P. and Faller D.V. (1991). Hypoxia induces endothelin gene expression and secretion in cultured human endothelium. *J. Clin. Invest.* 88, 1054-1057.
- Kudo H., Ueda H., Mochida K., Adachi S., Hara A., Nagasawa H., Doi Y., Fujimoto S. and Yamauchi K. (1999). Salmonid olfactory system-specific protein (N24) exhibits glutathione S-transferase class pi-like structure. *J. Neurochem.* 72, 1344-1352.
- McEver R.P., Beckstead J.H., Moore K.L., Marshall-Carison L. and Bainton D.F. (1989). GMP-140, a platelet -granule membrane

- protein, is also synthesized by vascular endothelial cells and is localized in Weibel-Palade bodies. *J. Clin. Invest.* 84, 92-99.
- McLean I.W. and Nakane P.K. (1974). Periodate-lysine-paraformaldehyde fixative: a new fixative for immunoelectron microscopy. *J. Histochem. Cytochem.* 22, 1077-1083.
- Meyrick B. and Reid L. (1978) The effect of continued hypoxia on rat pulmonary arterial circulation. An ultrastructural study. *Lab. Invest.* 38, 188-200.
- Opgenorth T.J., Wu-Wong J.R. and Shiosaki K. (1992). Endothelin-converting enzymes. *FASEB J.* 6, 2653-2659.
- Ozaka T., Doi Y., Kayashima K. and Fujimoto S. (1997). Weibel-Palade bodies as a storage site of calcitonin gene-related peptide and endothelin-1 in blood vessels of the rat carotid body. *Anat. Rec.* 247, 388-394.
- Pape D., Beuchard J., Guillo P., Allain H. and Bellissant E. (1997). Hypoxic contractile response in isolated rat thoracic aorta: role of endothelium, extracellular calcium and endothelin. *Fundam. Clin. Pharmacol.* 11, 121-126.
- Rakugi H., Tabuchi Y., Nakamaru M., Nagano M., Higashimori K., Mikami H., Ogihara T. and Suzuki N. (1990). Evidence for endothelin-1 release from resistance vessels of rats in response to hypoxia. *Biochem. Biophys. Res. Commun.* 169, 973-977.
- Rubanyi G.M. and Vanhoutte P.M. (1985). Hypoxia releases a vasoconstrictor substance from the canine vascular endothelium. *J. Physiol.* 364, 45-56.
- Russell F.D., Skepper J.N. and Davenport A.P. (1998a). Evidence using immunoelectron microscopy for regulated and constitutive pathways in the transport and release of endothelin. *J. Cardiovasc. Pharmacol.* 31, 424-430.
- Russell F.D., Skepper J.N. and Davenport A.P. (1998b). Human endothelial cell storage granules. a novel intracellular site for isoforms of the endothelin-converting enzyme. *Circ. Res.* 83, 314-321.
- Sakamoto Y., Doi Y., Ohsato K. and Fujimoto S. (1993). Immunoelectron microscopy on the localization of endothelin in the umbilical vein of perinatal rabbits. *Anat. Rec.* 237, 482-488.
- Shimada K., Takahashi M. and Tanzawa K. (1994). Cloning and functional expression of endothelin-converting enzyme from rat endothelial cells. *J. Biol. Chem.* 269, 18275-18278.
- Ueda H., Doi Y., Sakamoto Y., Hamasaki K. and Fujimoto S. (1992). Simultaneous localization of histamine and factor VIII-related antigen in the endothelium of the human umbilical vein. *Anat. Rec.* 232, 257-261.
- Weibel E.R. and Palade G.E. (1964). New cytoplasmic components in arterial endothelia. *J. Cell Biol.* 23, 101-112.
- Yanagisawa M., Kurihara H., Kimura S., Tomobe Y., Kobayashi M., Mitsui Y., Yazaki Y., Goto K. and Masaki T. (1988). A novel potent vasoconstrictor peptide produced by vascular endothelial cells. *Nature* 332, 411-415.
- Yoshizuka M., Tanaka I., Mori N., Maruyama T., Hirano T., Doi Y., Kawahara A., Miyazaki M. and Fujimoto S. (1990). Cadmium toxicity on the thoracic aorta of pregnant rats: electron microscopy and x-ray microanalysis. *Biomed. Res.* 1, 11-17.

Accepted September 11, 2001